International Journal of Mass Spectrometry 286 (2009) 83–88

Contents lists available at ScienceDirect

International Journal of Mass Spectrometry

journal homepage: www.elsevier.com/locate/ijms

Differentiation of the pyridine radical cation from its distonic isomers by ion–molecule reactions with dioxygen

Karl J. Jobst[a], Julien De Winter[b], Robert Flammang[b], Johan K. Terlouw[a], Pascal Gerbaux[b,*]

[a] Department of Chemistry, McMaster University, 1280 Main St. W., Hamilton, ON L8S 4M1,Canada
[b] Mass Spectrometry Center, Organic Chemistry Laboratory, University of Mons, 20 Place du Parc, B-7000 Mons, Belgium

ARTICLE INFO

Article history:
Received 25 May 2009
Received in revised form 19 June 2009
Accepted 22 June 2009
Available online 30 June 2009

Keywords:
Ion–molecule reactions
Isomer differentiation
Pyridine ylid
Model chemistry
Astrochemistry

ABSTRACT

In a previous study on the pyridine ion (**1**) and the pyridine-2-ylid isomer (**2**), we reported that ions **2** readily react with H_2O to produce 2-pyridone ions at *m*/*z* 95, by O-atom abstraction. The mechanism for this intriguing reaction, however, was not established. This prompted us to use model chemistry calculations (CBS-QB3) to probe various mechanistic scenarios and to perform complementary experiments with the new, more versatile, ion–molecule reaction chamber of the Mons Autospec 6F mass spectrometer. It appears that H_2O is not reacting neutral that produces the 2-pyridone ion of the above reaction, but rather O_2 from air co-introduced with the water vapour. Theory and experiment agree that the exothermic reaction of O_2 with the pyridine-2-ylid ion leads to loss of ^3O from a stable peroxide-type adduct ion at *m*/*z* 111. Similarly, pyridine-3-ylid ions (**3**) generate 3-pyridone ions, but the reaction in this case is thermoneutral. The *m*/*z* 111:95 peak intensity ratios in the spectra of the ion–molecule products from ions **2** and **3** may serve to differentiate the isomers.

1. Introduction

Differentiation of a gaseous organic ion from its isomers is commonly based upon high-energy collision-induced dissociation (CID) mass spectra of mass selected ions. However, this approach may be difficult or even impossible to realize if a set of isomeric ions only displays common dissociation pathways [1]. As an alternative, the reactivity of the ion under investigation may be probed by interactions with selected neutral molecules. Apart from charge exchange and protonation reactions, highly structure-specific associative ion–molecule reactions may occur, which readily distinguish the ion from its structural isomers [1]. This is especially true for distonic ions, because of their unique tendency to exhibit radical-type reactivity [2,3].

A case in point concerns our previous work [4a–c] on the pyridine ion and its distonic (1,2-H shift) isomers shown in Scheme 1. The distonic isomers are remarkably stable relative to ionized pyridine but are separated by high interconversion barriers. Consequently, these isomers can be differentiated on the basis of the *m*/*z* 28 ($HCNH^+$):26 ($C_2H_2{\cdot}^+$) peak intensity ratio in their high-energy CID mass spectra [4a,b].

However, an easier differentiation was achieved in our more recent study of this system [4c,5] by associative ion–molecule reactions involving a variety of neutral reagents, including H_2O. Neutral water does not react with the pyridine ion, but its α-distonic isomer was found to readily generate the 2-pyridone ion, by an O-atom transfer [4c].

The mechanism for this intriguing reaction, however, was not established. This prompted us to use model chemistry calculations (CBS-QB3) to probe various mechanistic scenarios and also to perform complementary experiments with the new, more versatile, ion–molecule reaction chamber of the Mons Autospec 6F instrument. It will be shown that H_2O is not reacting neutral that produces the 2-pyridone ion of the above reaction, but rather O_2 from air co-introduced with the water vapour in the ion–molecule reaction chamber.

2. Experimental methods

2.1. Tandem mass spectrometry

The experiments were performed on the Mons AutoSpec 6F (Waters, Manchester), a six-sector magnetic deflection instrument of EBEEBE geometry (E = Electric sector, B = Magnetic sector) [6a]. The instrument is equipped with four conventional collision chambers (C_{1-4}) to realize high-energy collision-induced dissociations; an early modification [6b] involved the installation of

* Corresponding author.
E-mail address: Pascal.Gerbaux@umh.ac.be (P. Gerbaux).

1387-3806/$ – see front matter © 2009 Elsevier B.V. All rights reserved.
doi:10.1016/j.ijms.2009.06.012

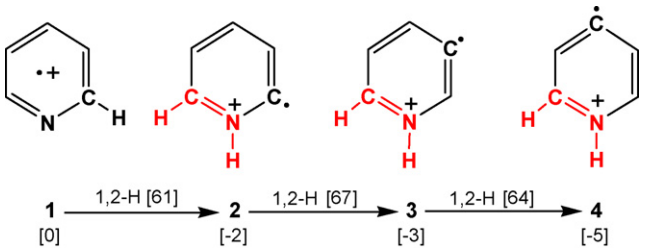

Scheme 1. Structures of the pyridine ion 1 and its α-, β- and γ-distonic isomers **2**–**4**. Relative energies are in kcal mol^{-1} and taken from Ref. [4].

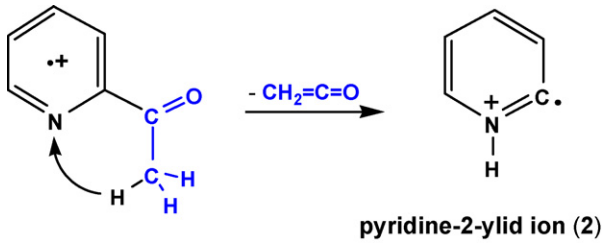

Scheme 2. The generation of pyridine-2-ylid ions by dissociative ionization of 2-acetylpyridine.

an rf-only quadrupole reaction chamber for studies of associative ion–molecule reactions.

This modification has recently been improved [6c] by replacing the quadrupole by a hexapole (HEX) setup so that the present configuration is: $C_1E_1B_1C_2E_2$–HEX–$C_3E_3B_2C_4E_4$.

The ions studied were generated by (dissociative) electron ionization (70 eV electrons, 200 μA trap current) and accelerated to 8 keV translational energy. The precursor molecules used are commercially available. They were introduced via a direct insertion probe (solids) or a heated septum inlet system at 160 °C (liquids).

In brief, the experiments of this study involve mass selection of a beam of fast moving ions (8 keV) using the first three sectors ($E_1B_1E_2$). Next, the ions are decelerated to circa 5 eV in front of the hexapole cell to optimize the yield of associative ion–molecule reactions with the neutral reagent—typically at a pressure of 4×10^{-4} mbar, as measured with a Pirani gauge located inside the cell. Following reacceleration to 8 keV, ions leaving the hexapole cell are mass analyzed by scanning the field of the second magnet. Finally, a given mass selected ion (using B_2) is subjected to collision-induced dissociation with N_2 in chamber C_4, and its CID mass spectrum is obtained by scanning sector E_4.

2.2. Computational methods

The calculations were performed using the Gaussian 03 Rev. C.02 and D.01 suite of programs [7] on SHARCNET. Enthalpies of formation ($\Delta_fH^0_{298}$ values in kcal mol^{-1}) for the various ions and neutrals in the Schemes and Table 1 were obtained from the CBS-QB3 model chemistry [8]. The identity of local minima and connecting transition states (TS) was confirmed by frequency analysis. Enthalpies derived from this and other model chemistries are expected to be of chemical accuracy (±2 kcal mol^{-1}). However, as pointed out by a reviewer, for the peroxy-type ions **D**2 and **D**3, the performance of the method may be compromised by an inadequate reference wave function.

The complete set of computational results including the optimized geometries is available from the authors upon request.

3. Results and discussion

3.1. The associative ion–molecule reaction of the pyridine-2-ylid ion with H_2O

Pyridine-2-ylid ions (**2**) are readily generated in the dissociative ionization of 2-acetylpyridine [5] by the route depicted in Scheme 2.

In good agreement with the results of our previous study [4c], the reaction of mass selected ions **2** with H_2O vapour in the hexapole reaction chamber of our mass spectrometer leads to the formation of *m*/*z* 95 product ions, as witnessed by the spectrum of Fig. 1a. Under the same conditions, pyridine ions (**1**) are unreactive.

The (high-energy) CID mass spectrum of these *m*/*z* 95 product ions, see Fig. 1d, is closely similar to that of the molecular ions produced in the EI mass spectrum of the 2-hydroxypyridine/pyridine-2-one system of tautomers [9]. This result, and the fact that the reaction with **D_2O** as the reagent exclusively generates *m*/*z* 95 ions, led to the proposal [4c] that the 2-pyridone ion

Table 1
Energetic data from CBS-QB3 calculations for the ion–molecule reactions of pyridine-2-ylid and pyridine-3-ylid ions described in Schemes 3 and 4 [a].

Structure	CBS-QB3 E(total) [0 K]	QB3 $\Delta_fH^0_{298}$	EXPT [b] $\Delta_fH^0_{298}$
Ion **1** (pyridine ion)	−247.49012	248	247
Ion **2** (pyridine-2-ylid ion)	−247.49103	247.5	–
Ion **3** (pyridine-3-ylid ion)	−247.49293	246	–
Ion **2** + H_2O	–	189 [c]	–
HBRC1	−323.85403	173	–
TS **HBRC**1 → 2		(194)	–
HBRC2	−323.846581	178	
Ion **D1**a	−323.86587	165	–
Protonated pyridine + •OH	–	187 [c]	
Protonated pyridine	−248.18185	178	
2-Pyridone ion + H_2	–	178	176
2-Pyridone ion	−322.68334	178	176
Ion **D**2	−397.72966	199	–
2-Pyridone ion + ^3O	–	237 [c]	236
TS 2-pyridone ion → pyrrole ion	−322.60929	283 [d]	
Pyrrole ion + CO + ^3O	–	249 [c]	248
Pyrrole ion	−209.48311	217	215
Ion **D**3	−397.72565	202	–
3-Pyridone ion + ^3O	–	246	–
TS 3-pyridone ion → pyrrole ion	−322.56735	310 [d]	
3-Pyridone ion	−322.66798	187	–

[a] $E_{(total)}$ in Hartrees, all other components are in kcal mol^{-1}; [b] Ref. [16]; [c] The CBS-QB3 derived enthalpies for H_2O, $^{\cdot}OH$, ^3O and CO are −58.2, 8.8, 59.4 and −26.9 kcal mol^{-1}; [d] The decarbonylation involves two transition states (ring-opening and loss of CO from the resulting intermediate) the quoted TS refers to the second step.

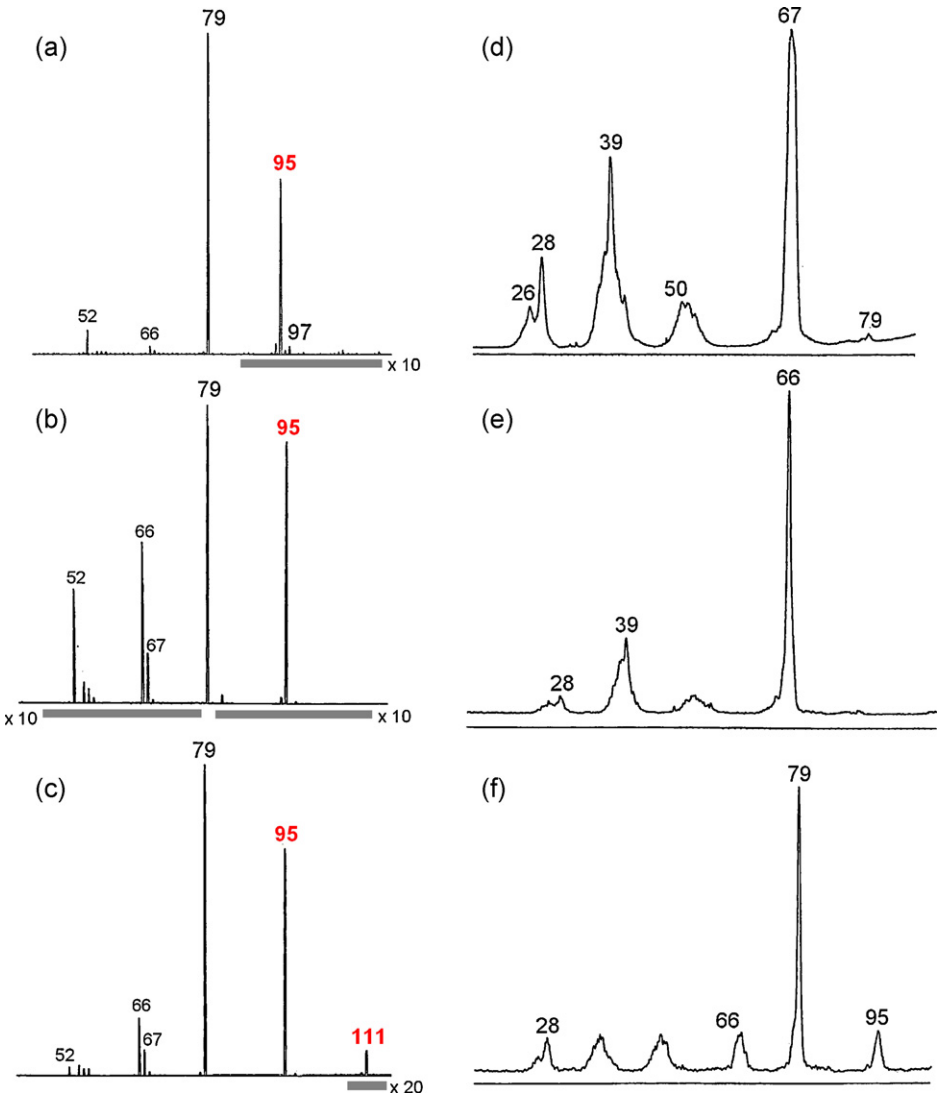

Fig. 1. Mass spectra of the products of the ion–molecule reactions of pyridine-2-ylid ions with: (a) water vapour; (b) dioxygen [O_2 pressure = 2×10^{-4} mbar] and (c) dioxygen [O_2 pressure = 8×10^{-4} mbar]. Items (d–f) are CID mass spectra of the *m*/*z* 95, *m*/*z* 94 and *m*/*z* 111 ions, generated in the above ion–molecule reaction with dioxygen.

is the major reaction product from the *m*/*z* 97 adduct ion comprised of H_2O and ion **2**.

The model chemistry calculations of Scheme 3 show that the interaction of a single water molecule with ion **2** may yield hydrogen-bridged radical cation **HBRC**1 [10]. This ion could be envisaged to isomerize into **D1**a or **D1**b but neither pathway appears to be energetically feasible:

(i) The isomerization of **HBRC**1 into **D1**a involves a prohibitively high TS at 197 kcal mol^{-1} for the formation of the intermediate ion **HBRC**2. This ion, see Table 1, is predicted to dissociate by loss of $OH^{\bullet}$ (which is not experimentally observed!) rather than rearrange into ion **D1**a.

(ii) Adduct ion **D1**b, generated by C–O bond formation, is not even a minimum. Finally, the subsequent 1,2- and 1,1-H_2 elimination reactions from **D1**a and **D1**b are expected to have considerable energy barriers.

Thus, despite the exothermicity of the reaction, the scenario of Scheme 3 predicts that the bulk of the *m*/*z* 97 adduct ions dissociate by loss of water. In line with this prediction, the *m*/*z* 97 adduct ions do not lose H_2 to any significant extent in their CID mass spectrum (not shown). Instead, these ions primarily back-dissociate into ions **2** and H_2O. It is therefore highly unlikely that the 2-pyridone ion is generated in the reaction of a water molecule with ion **2**.

This led us to consider the possibility that the 2-pyridone ion is generated by another reagent. A plausible candidate would be triplet (biradical) O_2 molecules from air co-introduced with the water vapour. Such a reaction would not be unprecedented: reactions of distonic ions and O_2 have been observed previously [11,12]. Indeed, a drawback of the present inlet system is that, despite multiple freeze/pump cycles, air may be co-introduced into the hexapole cell when dealing with reagents of low volatility. This prompted us to examine the interaction of pyridine-2-ylid ions with pure oxygen.

3.2. The associative ion–molecule reaction of the pyridine-2-ylid ion (**2**) with dioxygen

Fig. 1b shows the mass spectrum of the products of the ion–molecule reaction of pyridine-2-ylid ions (*m*/*z* 79) and pure oxygen. That 2-pyridone ions are readily generated in the reaction is revealed by the intense peak at *m*/*z* 95 and its corresponding CID mass spectrum, which is identical with that shown in Fig. 1d.

These observations are rationalized by the model chemistry calculations of Scheme 4a, which show that the initial interaction between ion **2** and O_2 leads to the remarkably stable covalently

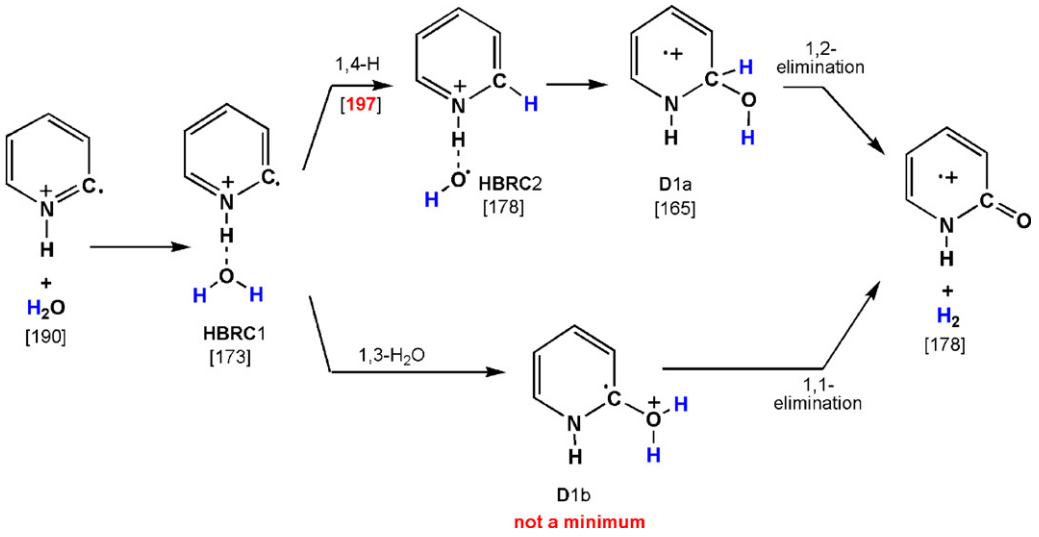

Scheme 3. The ion–molecule reaction of the pyridine-2-ylid ion 2 with H_2O. The numbers refer to 298 K enthalpies in kcal mol^{-1} derived from CBS-QB3 calculations.

bound species **D**2. This peroxide-type ion enjoys considerable stabilization, c. 50 kcal mol^{-1}, relative to the combined enthalpies of ion **2** and O_2. Our calculations further show that loss of ^3O from ion **D**2 yields the 2-pyridone ion in a process that is continuously exothermic by 11 kcal mol^{-1} relative to the combined enthalpies of ion **2** and O_2.

The spectrum of Fig. 1b also shows peaks at *m*/*z* 52, 66 and 67, whose formation deserves comment. The signal at *m*/*z* 52 ($C_4H_4^{\cdot+}$) is readily attributed to the spontaneous and collision-induced loss of HCN from the mass selected 2-ylid ions [4a], but the other two ions must result from associative ion–molecule reactions between the 2-ylid ion and O_2.

The *m*/*z* 67 ion, readily identified as the pyrrole ion on the basis of its CID mass spectrum (not shown), likely originates from decarbonylating 2-pyridone ions: see the CID mass spectrum of Fig. 1d, where *m*/*z* 67 is the base peak. The calculated TS for the decarbonylation is quite high (283 kcal mol^{-1}), in line with the results of a previous study on isomeric $C_5H_5NO^+$ ions [9].

This raises the question as to why this energy demanding reaction is observed. First, we note that the EI generated 2-ylid reactant ions may have up to ~70 kcal mol^{-1} of internal energy, the estimated energy requirement for the spontaneous loss of HCN [4a,d]. Thermalization of these ions by (unreactive) collisions with the neutral reagent takes place in the hexapole cell but this process may be rather inefficient in our experimental set-up. Perhaps more likely, ions entering the hexapole cell have a minimum translational energy of ~5 eV, so that collision-induced dissociation may still compete with collisional cooling. In line with this, Fig. 1c shows that the relative intensity of the *m*/*z* 67 (and *m*/*z* 52) peak decreases considerably when the O_2 pressure is raised.

The spectrum of Fig. 1c indicates that the *m*/*z* 66 ion also results from a high-energy process. Its CID mass spectrum (not shown)

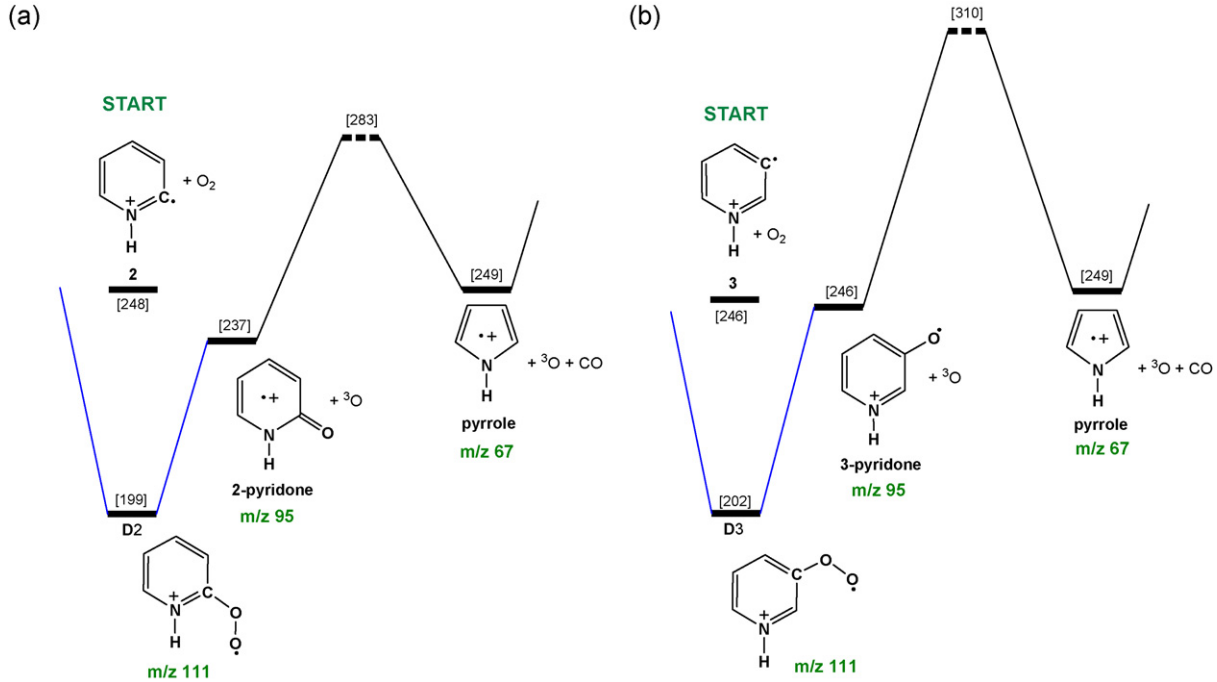

Scheme 4. Potential energy diagrams describing the associative ion–molecule reactions of (a) the pyridine-2-ylid ion 2 and (b) the pyridine-3-ylid ion 3 with dioxygen. Numbers in square bracket refer to CBS-QB3 derived 298 K enthalpies in kcal mol^{-1}.

may be that of a $C_4H_4N^+$ isomer for which, unfortunately, reference spectra are not available. Several pathways for its formation can be envisaged, but in the absence of further information, these remain highly speculative. The CID mass spectrum of Fig. 1e, indicates that one route may involve decarbonylation of the weakly detected *m*/*z* 94 ions in the spectrum of Fig. 1b.

The most important feature of Fig. 1c is that at the elevated O_2 pressure, the *m*/*z* 111 adduct ion (**D**2) becomes observable. The fact that its CID mass spectrum shows a significant peak at *m*/*z* 95, see Fig. 1f, underlines our proposal that dioxygen, rather than water, reacts with the pyridine-2-ylid ion.

3.3. The associative ion–molecule reaction of the pyridine-3-ylid ion (**3**) with dioxygen

We have also studied the reaction of pyridine-3-ylid ions **3** with dioxygen to see if the distonic isomers **2** and **3** can be differentiated. Ions **3** can conveniently be generated by the dissociative ionization of 2,3-diacetylpyridine, as depicted in Scheme 5.

In line with the calculations of Scheme 4b, which predict that the O-atom abstraction of dioxygen by the radical site of ion **3** is a thermoneutral reaction, Fig. 2a displays a sizeable peak at *m*/*z* 95 for the reaction of ion **3** with dioxygen.

The CID mass spectrum of these *m*/*z* 95 ions is shown in Fig. 2c. The spectrum is virtually the same as that of the 3-pyridone ions generated by demethylation of protonated 3-methoxy-pyridine [9]. However, the CID mass spectra of 2- and 3-pyridone reported in Ref. [9] are closely similar and the same obtained for the CID spectra of Figs.1d and 2c.

Thus, ions **2** and **3** cannot be differentiated on the basis of the CID mass spectra of the *m*/*z* 95 ions. However, there is a striking difference in the relative abundance of the *m*/*z* 111 and 95 ions generated in the two reactions. Comparison of Figs.1b and 2a shows that at a relatively low O_2 pressure, the *m*/*z* 111 adduct ion is observed with ion **3** but not with ion **2**. This is in agreement with our calculations, namely that the O-atom abstraction is exothermic for ion **2** and thermoneutral for ion **3**. Thus, incipient ions **D**2 are more prone to dissociate prior to collisional stabilization than ions **D**3. This trend is paralleled in the mass spectra of Figs.1c and 2b where a higher oxygen pressure was used in the hexapole cell. The *m*/*z* 111:95 peak intensity ratio may therefore serve to differentiate ions **2** and **3**.

Finally, we note that adduct ions **D**2 or **D**3 are unlikely to further react with O_2 under our experimental conditions. Exploratory calculations indicate that the reaction of **D**2 with O_2 is exothermic (by c. 15 kcal mol^{-1}), and that dissociation of the resulting [**D**2–O=O]$^{\cdot+}$ adduct ion into 2-pyridone$^{\cdot+}$ + O_3 is more energy demanding (by c. 25 kcal mol^{-1}) than back-dissociation into **D**2 + O_2.

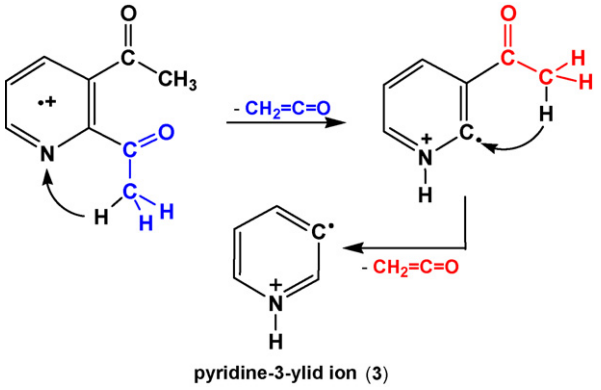

Scheme 5. The generation of pyridine-3-ylid ions by dissociative ionization of 2,3-diacetylpyridine.

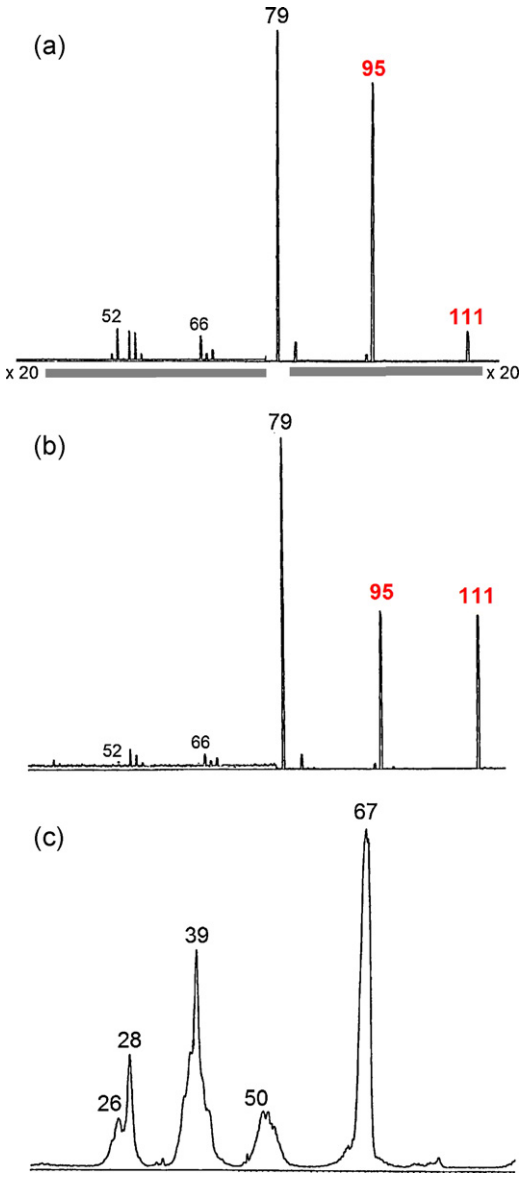

Fig. 2. Mass spectra of the products of the ion–molecule reactions of pyridine-3-ylid ions with dioxygen. (a) [O_2 pressure = 2×10^{-4} mbar] and (b) [O_2 pressure = 8×10^{-4} mbar]; (c) CID mass spectrum of the *m*/*z* 95 ions generated in the above ion–molecule reaction.

4. Conclusions

The previously reported [4c] formation of the 2-pyridone ion from the pyridine-2-ylid ion and H_2O appears to refer to the reaction of O_2 from air co-introduced with the water vapour. Theory and experiment agree that this exothermic reaction leads to loss of ^3O from a stable peroxide-type adduct ion at *m*/*z* 111. Similarly, pyridine-3-ylid ions (**3**) generate 3-pyridone ions, but the reaction in this case is thermoneutral. The *m*/*z* 111:95 peak intensity ratios in the spectra of the ion–molecule products from ions **2** and **3** reflect the different energy requirements and may serve as a diagnostic tool to differentiate the isomers.

The reported O-atom abstraction may well represent a general reaction of distonic heterocyclic ions: work in progress shows that the distonic ions of pyrimidine [13], imidazole [14] and thiazole [14] show the same behaviour. The reaction of O_2 with the distonic ions of the prebiotic pyrimidine molecule may be of interest to astrochemistry [15].

Acknowledgements

PG (Research Associate), RF and JDW (Research Fellow) are grateful to the "Fonds pour la Recherche Scientifique" (FRS-FNRS) for financial support in the acquisition of the Waters AutoSpec 6F and for continuing support. JKT and KJJ thank the Natural Sciences and Engineering Research Council of Canada (NSERC) for financial support, SHARCNET for the computational resources and Dr. P.C. Burgers for valuable discussions.

References

[1] J.L. Holmes, C. Aubry, P.M. Mayer, Assigning Structures to Ions in Mass Spectrometry, CRC Press, Boca Raton, FL, 2007.
[2] K.M. Stirk, L.K.M. Kiminkinen, H.I. Kenttämaa, Chem. Rev. 92 (1992) 1649.
[3] (a) J.S. Brodbelt, Mass Spectrom. Rev. 16 (1997) 91;
(b) S. Gronert, Chem. Rev. 101 (2001) 329;
(c) P. Gerbaux, P. Wantier, P.N. Cam, M.T. Nguyen, G. Bouchoux, R. Flammang, Eur. J. Mass Spectrom. 10 (2004) 889;
(d) Y.E. Corilo, M.N. Eberlin, J. Mass Spectrom. 43 (2008) 1636.
[4] (a) D. Lavorato, J.K. Terlouw, T.K. Dargel, W. Koch, G.A. McGibbon, H. Schwarz, J. Am. Chem. Soc. 118 (1996) 11898;
(b) D. Lavorato, J.K. Terlouw, T.K. Dargel, G.A. McGibbon, W. Koch, H. Schwarz, Int. J. Mass Spectrom. 179/180 (1998) 7;
(c) P. Gerbaux, M. Barbieux-Flammang, J.K. Terlouw, R. Flammang, Int. J. Mass Spectrom. 206 (2001) 91;
(d) P.C. Burgers, J.L. Holmes, Int. J. Mass Spectrom. Ion Processes 58 (1984) 15.
[5] P. Gerbaux, M. Barbieux-Flammang, Y. Van Haverbeke, R. Flammang, Rapid Commun. Mass Spectrom. 13 (1999) 1707.
[6] (a) R.H. Bateman, J. Brown, M. Lefevere, R. Flammang, Y. Van Haverbeke, Int. J. Mass Spectrom. Ion Processes 115 (1992) 205;
(b) R. Flammang, Y. Van Haverbeke, C. Braybrook, J. Brown, Rapid Commun. Mass Spectrom. 9 (1995) 795;
(c) L. Trupia, N. Dechamps, R. Flammang, G. Bouchoux, M.T. Nguyen, P. Gerbaux, J. Am. Soc. Mass Spectrom. 19 (2008) 126.
[7] M.J. Frisch, G.W. Trucks, H.B. Schlegel, G.E. Scuseria, M.A. Robb, J.R. Cheeseman, J.A. Montgomery Jr., T. Vreven, K.N. Kudin, J.C. Burant, J.M. Millam, S.S. Iyengar, J. Tomasi, V. Barone, B. Mennucci, M. Cossi, G. Scalmani, N. Rega, G.A. Petersson, H. Nakatsuji, M. Hada, M. Ehara, K. Toyota, R. Fukuda, J. Hasegawa, M. Ishida, T. Nakajima, Y. Honda, O. Kitao, H. Nakai, M. Klene, X. Li, J.E. Knox, H.P. Hratchian, J.B. Cross, V. Bakken, C. Adamo, J. Jaramillo, R. Gomperts, R.E. Stratmann, O. Yazyev, A.J. Austin, R. Cammi, C. Pomelli, J.W. Ochterski, P.Y. Ayala, K. Morokuma, G.A. Voth, P. Salvador, J.J. Dannenberg, V.G. Zakrzewski, S. Dapprich, A.D. Daniels, M.C. Strain, O. Farkas, D.K. Malick, A.D. Rabuck, K. Raghavachari, J.B. Foresman, J.V. Ortiz, Q. Cui, A.G. Baboul, S. Clifford, J. Cioslowski, B.B. Stefanov, G. Liu, A. Liashenko, P. Piskorz, I. Komaromi, R.L. Martin, D.J. Fox, T. Keith, M.A. Al-Laham, C.Y. Peng, A. Nanayakkara, M. Challacombe, P.M.W. Gill, B. Johnson, W. Chen, M.W. Wong, C. Gonzalez, J.A. Pople, Gaussian 03, Revision C.02/D.01, Gaussian Inc., Wallingford, CT, 2004.
[8] J.A. Montgomery Jr., M.J. Frisch, J.W. Ochterski, G.A. Petersson, J. Chem. Phys. 112 (2000) 6532.
[9] M.A. Trikoupis, P. Gerbaux, D.J. Lavorato, R. Flammang, J.K. Terlouw, Int. J. Mass Spectrom. 217 (2002) 1.
[10] P.C. Burgers, J.K. Terlouw, in: N.M.M. Nibbering (Ed.), Encyclopedia of Mass Spectrometry, vol. 4, Elsevier, Amsterdam, 2005, p. 173.
[11] S.J. Yu, C.L. Holliman, D.L. Rempel, M.L. Gross, J. Am. Chem. Soc. 115 (1993) 9676.
[12] (a) P.G. Wenthold, J. Hu, R.R. Squires, J. Mass Spectrom. 33 (1998) 796;
(b) D.G. Harman, S.J. Blanksby, Org. Biomol. Chem. 5 (2007) 3495.
[13] D.J. Lavorato, T.K. Dargel, W. Koch, G.A. McGibbon, H. Schwarz, J.K. Terlouw, Int. J. Mass Specrom. 210/211 (2001) 43.
[14] R. Flammang, M.T. Nguyen, G. Bouchoux, P. Gerbaux, Int. J. Mass Spectrom. 202 (2000) A8.
[15] H.K. Ervasti, K.J. Jobst, P.C. Burgers, P.J.A. Ruttink, J.K. Terlouw, Int. J. Mass Spectrom. 262 (2007) 88.
[16] S.G. Lias, J.E. Bartmess, J.F. Liebman, J.L. Holmes, R.D. Levin, W.G. Mallard, J. Phys. Chem. Ref. Data 17 (Suppl. 1) (1988).